

Examination of Soil Microbial Communities After Permafrost Thaw Subsequent to an Active Layer Detachment in the High Arctic

Authors: Inglese, Cara N., Christiansen, Casper T., Lamhonwah, Daniel, Moniz, Kristy, Montross, Scott N., et al.

Source: Arctic, Antarctic, and Alpine Research, 49(3) : 455-472

Published By: Institute of Arctic and Alpine Research (INSTAAR), University of Colorado

URL: <https://doi.org/10.1657/AAAR0016-066>

BioOne Complete (complete.BioOne.org) is a full-text database of 200 subscribed and open-access titles in the biological, ecological, and environmental sciences published by nonprofit societies, associations, museums, institutions, and presses.

Your use of this PDF, the BioOne Complete website, and all posted and associated content indicates your acceptance of BioOne's Terms of Use, available at www.bioone.org/terms-of-use.

Usage of BioOne Complete content is strictly limited to personal, educational, and non - commercial use. Commercial inquiries or rights and permissions requests should be directed to the individual publisher as copyright holder.

BioOne sees sustainable scholarly publishing as an inherently collaborative enterprise connecting authors, nonprofit publishers, academic institutions, research libraries, and research funders in the common goal of maximizing access to critical research.

Examination of soil microbial communities after permafrost thaw subsequent to an active layer detachment in the High Arctic

Cara N. Inglese^{1,4,*}, Casper T. Christiansen^{1,5}, Daniel Lamhonwah², Kristy Moniz¹, Scott N. Montross², Scott Lamoureux^{2,3}, Melissa Lafrenière², Paul Grogan¹, and Virginia K. Walker^{1,3}

¹Department of Biology, Queen's University, 116 Barrie Street, Kingston, Ontario, K7L 3N6, Canada

²Department of Geography and Planning, Queen's University, 68 University Avenue, Kingston, Ontario, K7L 3N6, Canada

³School of Environmental Studies, Queen's University, 116 Barrie Street, Kingston, Ontario, K7L 3N6, Canada

⁴Present address: B.C. Women's Hospital and Health Center, Provincial Medical Genetics Program, 4500 Oak Street, Vancouver, British Columbia, V6H 3N1, Canada

⁵Present address: Uni Research Climate, Nygårdsgaten 112, 5008 Bergen, Norway

*Corresponding author's email: cara.inglese@cw.bc.ca

ABSTRACT

Active layer detachments (ALDs) are permafrost disturbances associated with climate change and increased seasonal warming. Such perturbations result from thawing of the upper permafrost and downslope movement of the overlying thawed material, including the active layer. ALDs have the potential to impact soil microbial community composition and function in arctic soil ecosystems. Here we report an initial investigation of an ALD located at Cape Bounty on Melville Island in the Canadian High Arctic. We examined soil nutrient content as well as microbial community structure using denaturing gradient gel electrophoresis and sequencing. Soil from the disturbed site showed changes in microbial communities with strikingly different fungal community composition compared to soils from an adjacent undisturbed site. These community changes were correlated with enhanced levels of dissolved organic carbon, microbial carbon, total dissolved nitrogen, and microbial nitrogen. The Nitrososphaerales—an order of ammonia-oxidizing Archaea—were more abundant in the disturbed soil and may have been responsible for the altered nitrogen cycling that resulted in higher levels of total dissolved nitrogen there. The fungal communities at both sites were dominated by orders within the Ascomycota, a phylum of mainly hyphal fungi. Intriguingly however, they were more numerous in the undisturbed soil compared to the disturbed soil, suggesting that certain Ascomycota could not reestablish within six years of the ALD, and more generally that fungal hyphal networks may help to stabilize tundra surface soils against erosional losses.

INTRODUCTION

Some areas of the Canadian High Arctic are already on track to follow predictions that there will be a 4–8 °C increase in average air temperature within this century (IPCC, 2007). Thus, it is not surprising to learn that the permafrost, which comprises a significant proportion of the terrestrial landscape, is warming and thawing,

resulting in disturbances and changing soil conditions (Lamoureux and Lafrenière, 2009; Yergeau et al., 2010; Pautler et al., 2010). This thawing can result in ecosystem- and landscape-scale disturbances such as thermokarst (including collapsed pingos and sinkholes), as well as disturbances including active layer detachments (ALDs) and larger retrogressive thaw slumps (Jones et al., 2013). Such permafrost disturbances are of interest

to civil authorities because infrastructure is at risk, but they are also of ecological concern with implications for carbon storage, vegetation changes, sediment erosion, ecosystem function, and nutrient cycling, among other impacts. In ALDs, an accumulation of water at the active layer–permafrost boundary, in combination with a slightly sloped topography, is thought to result in the sliding of a thawed active-layer horizon (Lamoureux and Lafrenière, 2009). After an ALD, the former upper permafrost (and carbon and nutrients within) is exposed, thus subjecting microbial communities to more extreme temperature variations, and changes in moisture, nutrient, and oxygen content, which have been shown to result in higher concentrations of bacterial and fungal fatty acid phospholipids (Pautler et al., 2010).

In High Arctic soils, the dominant bacterial phyla include Acidobacteria, Proteobacteria, and Gemmatimonadetes, although archaeal communities show less diversity in both the active layer and permafrost (Wilhelm et al., 2011). Fungi can dominate such ecosystems, particularly in the winter (Schadt et al., 2003; Buckeridge et al., 2013), and consist of both single cellular fungi such as yeasts and macroscopic filamentous fungi with hyphae from all the major phyla: Ascomycota, Basidiomycota, Zygomycota, Chytridiomycota, and Glomeromycota (Wagner, 2008; Timling and Taylor, 2012). Such communities are impacted by a variety of abiotic factors. For example, arctic fungal communities differ with soil pH, C:N ratio, and available phosphorus as well as in association with frost heave and long-term experimental warming (Fujimura and Egger, 2012; Timling et al., 2014; Geml et al., 2015). Together, however, these various bacteria, Archaea, and fungi perform key functions in global biogeochemical cycling, including nitrogen cycling. Thus, any changes in microbial assemblages following ALDs could have important consequences for soil function and nutrient availability to plants, and yet these effects have been largely unexplored.

On Melville Island in Canada's High Arctic, the seasonally thawed soil active layer comprises the top ~50–90 cm and is underlain by continuous permafrost (Steven et al., 2007; Wilhelm et al., 2011). During the summer of 2007, there was an uncharacteristically high mean July temperature of 10.8 °C, relative to the 2003–2006 mean July temperature of 4.0 °C (Pautler et al., 2010), and this thermal perturbation, as well as unusually heavy rainfall, resulted in numerous ALDs. It is expected that such permafrost disturbances will increase in frequency as regional climate warming continues (Lamoureux and Lafrenière, 2009). We hypothesized that the ALDs would alter soil assemblages as assessed by molecular phylogenetic approaches including denaturing gradient gel electrophoresis (DGGE) and pyrosequence

analysis. This report represents an initial examination of the impact of an active layer slide, which we hope will serve as a model to encourage additional studies at other High Arctic sites, as well as provide baseline information for models of expected changes in soil functioning due to ALDs in arctic environments.

MATERIALS AND METHODS

Study Site and Sampling Protocol

The Cape Bounty Arctic Watershed Observatory (CBAWO) is located on Melville Island, Nunavut, in the Canadian High Arctic (74°54'N, 109°35'W). The active layer typically reaches a maximum of ~90 cm in early August and overlies thick, continuous permafrost. The climate is characterized by mean annual precipitation of 160 mm, with the majority falling as snow, and with a mean annual temperature of –17.5 °C (Lewis and Lamoureux, 2010). Indeed, historically, temperatures range between 0 and 4 °C in June and September. However, in the first two weeks of July 2007 there was an uncharacteristically warm period with daily maximum temperatures rising above 20 °C and resulting in an overall mean July air temperature of 10.8 °C, compared to means of 4.0 °C in previous years (Lamoureux and Lafrenière, 2009). There were also unusual rainfall events in 2007, which increased the potential for ground ice to thaw in the CBAWO compared to other years (Lamoureux and Lafrenière, 2009). These unusual conditions culminated in a period of ALD formation that ultimately affected ~3% of the total area of the West River watershed at CBAWO (Lewis et al., 2012).

Two soil cores were obtained from the West River watershed, which is characterized by mesic High Arctic vegetation, on 17–19 May 2013 (i.e. in late winter while the soils were still frozen and six years after the disturbance). The dominant vascular plant species at both the disturbed and undisturbed coring locations were *Ranunculus nivalis*, *Potentilla vahliana*, *Salix arctica*, *Saxifraga oppositifolia*, and *Saxifraga tricuspidata* (Bosquet, 2011). One core (referred to as the disturbed core) was obtained at a site within the upper scar zone of the field marker (designated ALD-02 at CBAWO; Fig. 1). A second core (referred to as the undisturbed core) was located 8 m upslope from the disturbed core site above the head scarp in undisturbed soil (Fig. 1). Unfortunately, because of the remote geography and severe weather, further coring was not possible in 2013 or during the following 2014 season. During soil coring in the field, the top 13 cm of the undisturbed core did not remain intact due to its low bulk density and thus it crumbled during excavation and could not be retrieved or trans-

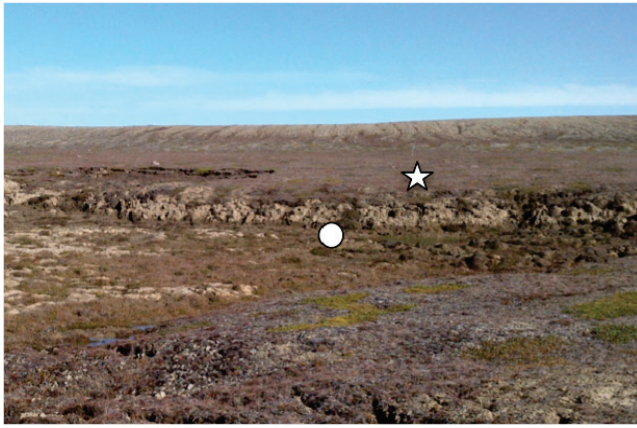


FIGURE 1. Photograph of the sampling location located near the head scarp of ALD02 at the Cape Bounty Arctic Watershed Observatory, showing disturbed and undisturbed sites. The photograph was taken in August 2015, two years after the cores were obtained. The circle is at the point of the disturbed coring site, and the star represents the undisturbed coring site. View northeast. Photographer: S. Lamoureux.

ported from the field. As a result, the top of the undisturbed core was annotated as 13 cm depth. Cores were kept frozen while transported and stored at -20°C . To avoid contamination, cores were subsampled in a walk-in -20°C freezer by scraping off the outer 5 mm of the cores with a small flame-sterilized metal blade. Then using a sterilized auger bit (1 cm diameter), a 5 mm hole was drilled into the cores at the location that the cores had been blade scraped, with soil obtained in both these procedures then discarded. Finally, the cores were drilled ~ 3 cm with a freshly sterilized bit, and soil subsample material caught in sterile aluminum foil. Starting at the top of each core, subsamples were retrieved using this procedure every ~ 5 cm. After transfer to a sterile plastic tube (50 mL), all subsamples were stored at -20°C until genomic DNA extraction.

Soil Biogeochemistry

Soil material from each sampling depth was thawed and homogenized, removing stones in the process. Afterward, the samples were subjected to chloroform-fumigation (Brookes et al., 1985). Briefly, each homogenized sample (10 g) was extracted with 0.5 M K_2SO_4 (1:5 fw:vw ratio) to recover soluble inorganic nutrients $\text{NH}_4^+\text{-N}$, $\text{NO}_3^-\text{-N}$, and $\text{PO}_4^{3-}\text{-P}$, and soluble organic carbon and nitrogen pools (DOC and TDN, respectively). The soil slurries were shaken for 1 h, allowed to settle for 30 min, and subsequently filtered (Fisher G4;

1.2 μm pore size). Another set of thawed and homogenized soil subsamples (10 g) were vacuum-incubated with ethanol-free chloroform (CHCl_3) for 24 h at $\sim 20^{\circ}\text{C}$, followed by immediate K_2SO_4 extraction (Buckridge and Grogan, 2010), as described above, to estimate microbial biomass pools of carbon, nitrogen, and phosphorus (MBC, MBN, and MBP, respectively; see microbial biomass calculations below). To detect potential contamination, we always included duplicate blanks for each extraction. For all samples, the extracted and filtered volume was immediately frozen at -20°C until further analysis.

From the K_2SO_4 extracts (CHCl_3 -fumigated and non-fumigated samples), DOC and TDN were determined by oxidative combustion and infrared (DOC; Nelson and Sommers, 1996) or chemiluminescence (TDN) analysis, using a TOC-TN Auto-Analyzer (Shimadzu, Kyoto, Japan). Dissolved $\text{NH}_4^+\text{-N}$ (non-fumigated extracts), $\text{NO}_3^-\text{-N}$ (non-fumigated extracts), and $\text{PO}_4^{3-}\text{-P}$ (fumigated and non-fumigated extracts) were all determined colorimetrically using automated flow analysis on an Auto-Analyzer III (Bran-Leubbe, Norderstadt, Germany), and the salicylate ($\text{NH}_4^+\text{-N}$; Mulvaney, 1996), sulphanimide ($\text{NO}_3^-\text{-N}$; Mulvaney, 1996), and ascorbic acid ($\text{PO}_4^{3-}\text{-P}$; Kuo, 1996) methods. Microbial biomass C, N, and P (MBC, MBN, and MBP, respectively) were calculated as the difference between DOC, TDN, and $\text{PO}_4^{3-}\text{-P}$ in fumigated and non-fumigated samples, while soluble organic nitrogen (DON) was calculated as $\text{TDN} - (\text{NH}_4^+\text{-N} + \text{NO}_3^-\text{-N})$. No correction factors for microbial extraction efficiencies were applied to the fumigated samples. All extractions were corrected for dilution associated with gravimetric soil moisture content of each sample (see below). All $\text{NH}_4^+\text{-N}$, $\text{NO}_3^-\text{-N}$, and $\text{PO}_4^{3-}\text{-P}$ (including MBP) measurements in the 0.5 M K_2SO_4 extracts were below detection limit and therefore are not reported.

Gravimetric soil moisture was determined by drying a third set of soil subsamples (10 g) at 60°C for 96 h. The dried samples were subsequently homogenized to a fine powder in a ball mill before determining total C and N by combustion on a VARIO Micro Cube (Elementar Analysensysteme, Hanau, Germany).

Samples for ion analysis were obtained by sampling the frozen cores at -20°C using a hammer and chisel that had been cleaned using ethanol and water. These samples were then dried for 24 h at 110°C and weighed. Following a previously published protocol (Kokelj and Burn, 2005), soluble ions were extracted following hydration with deionized water (2 g soil in 4 mL). The extracts were filtered using polyvinylidene fluoride membrane disks (13 mm 0.22 μm ; Sigma-Aldrich) fitted to 3 mL syringes. The filtrates were diluted 10-fold with deionized water

prior to analyses. Anion (Cl^- , Br^- , SO_4^{2-} , NO_2^- , NO_3^-) and cation (Li^+ , Na^+ , K^+ , Mg^{2+} , Ca^{2+} , Sr^{2+}) concentrations were quantified using liquid ion chromatography with a simultaneous injection dual pump Dionex ICS-3000 system. Anions were determined with a KOH gradient elution (11–40 mM KOH flowing at 1.0 mL min^{-1}) using the AS18 analytical column and an ASRS 300 suppressor. Cations were measured isocratically (ppm) after eluting with methane sulphonic acid (16 mM at 0.5 mL min^{-1}) from a CS12A-5 analytical column and a CSRS 300 suppressor. Detection limits were calculated as three times the standard deviation of replicates of standards containing low ion levels; these were routinely <0.005 ppm except for Mg^{2+} (0.016 ppm) and Ca^{2+} (0.039 ppm). The analytical uncertainty, based on replicates of internal method checks for anions and cations, was between 0.001 and 0.005 ppm for most ions, with the exception of Mg^{2+} (0.01 ppm) and Cl^- (0.008 ppm).

DNA Extraction

Each soil sample was ground to a fine powder in liquid nitrogen using a mortar and pestle (30 s). Genomic DNA was isolated from the ground soil (250 mg) using a NucleoSpin Soil DNA Isolation kit (Macherey-Nagel Inc., Bethlehem, Pennsylvania, U.S.A.), according to the manufacturer's instructions. Extractions were done in duplicate and pooled to yield sufficient DNA ($\sim 2 \mu\text{g}$) for multiple polymerase chain reaction (PCR) experiments. The concentration and purity of genomic DNA in each sample was determined using a NanoDrop spectrophotometer (NanoDrop-1000; Ver. 3.7.1) before PCR and subsequently examined using agarose gel electrophoresis (see below).

Polymerase Chain Reaction-Denaturing Gradient Gel Electrophoresis (PCR-DGGE)

PCR amplification of the bacterial and archaeal 16S and fungal 18S rRNA gene fragment was performed on extracted genomic DNA for DGGE analysis. PCR reaction mixtures (total volume of $50 \mu\text{L}$) were prepared with 2.5 U Taq polymerase (VPQ Scientific, Oceanside, California, U.S.A.), 0.01 mM of each deoxynucleoside triphosphate (dNTP), 0.5 nM of each primer, $400 \mu\text{g mL}^{-1}$ bovine serum albumin, and $5 \mu\text{L}$ of $10\times$ PCR buffer (160 mM $(\text{NH}_4)_2\text{SO}_4$, 500 mM Tris-HCl; pH 9.2 at 22°C), 17.5 mM MgCl_2 , and 0.1% Triton X-100, using 5–10 μL DNA template. A nested PCR method was used to generate fragments for archaeal and fungal DGGE analysis (Boon et al., 2002; Vissers et al., 2009). Primers and cycling conditions are listed in Table 1.

The PCR products were examined by electrophoresis on 1% agarose gels (Delidow et al., 1993), and if they were of the appropriate size and showed no spurious bands, the amplified DNA was then separated using a DGGE apparatus from C.B.S. Scientific (Del Mar, California, U.S.A.) according to standard procedures and the manufacturer's recommendations (Myers et al., 1988; Abrams and Stanton, 1992). Amplified DNA fragments were separated on 8% (w/v) polyacrylamide gel with a denaturing gradient of 35%–70% for bacterial, 40%–70% for archaeal, and 30%–60% for fungal samples (where 100% denaturing solution consisted of 7 M urea and 40% formamide). To visualize the chemical gradient on the gel, 400 μL of Dcode dye (0.5% bromophenol blue, 0.5% xylene cyanol, in $10 \text{ mL } 1\times$ Tris-Acetate-EDTA (TAE) buffer was added to the higher concentration of denaturing solution. The gels were electrophoresed at 120 V for 5 min, followed by 70 V for 20 h, in $1\times$ TAE buffer at 60°C . After electrophoresis, the gels were stained in $1\times$ TAE containing $0.05 \mu\text{g mL}^{-1}$ of ethidium bromide, and then photographed under UV light ($\sim 302 \text{ nm}$). PCR-DGGE was performed three or more times on each amplified sample to ensure the reproducibility of the gel patterns.

DNA Sequencing and Analysis

As indicated, cores were sampled every 5 cm, however, financial constraints prohibited the DNA analysis of all of these samples. Thus, after examining the DGGE profiles of each depth in both cores, a decision to sequence the genomic DNA was made if the band profile appeared to be unique relative to adjoining sample depths. Efforts were also made to sequence approximately corresponding depths in the two cores. Depths chosen for sequence analysis from the disturbed core were 1 cm (referred to as “top”), 16 cm, 26 cm, and 34 cm. The depths chosen for the undisturbed core corresponded at 16 cm, 26 cm, and 34 cm, but it must be noted that the shallowest sample or “top” sample from the undisturbed core was necessarily the uppermost soil that could be obtained from the crumbly surface at 13 cm (see sample collection). Genomic DNA extracted from these soil samples was subjected to bacterial tag-encoded FLX amplicon pyrosequencing (bTEFAP) according to standard methods (Molecular Research, MR DNA, Shallowater, Texas, U.S.A.). The sequencing library was generated by amplification of sequences corresponding to bacterial and archaeal 16S and fungal 18S rRNA regions (Table 1). Briefly, after bead purification, the amplified products were sequenced using the Genome Sequencer FLX System (Roche, Nutley, New Jersey, U.S.A.) with titanium reagents as previously described

TABLE 1

Conditions and primers used in PCR, sequencing, and qRT-PCR reactions.

Gene fragment	Primer sequence (5'-3')	Cycling conditions			Reference
		Denaturation	Annealing	Extension	
Bacterial 16S rRNA	PRBA338f-GC ^a primer 2	30 ^b 95 °C	45 s 64 °C	1 min 72 °C	3 min Øvreås et al. (1997) Muyzer et al. (1993)
Archaeal 16S rRNA	21F	15 ^b 95 °C	30 s 54 °C	45 s 72 °C	1 min Visser et al. (2009)
outer primer pair	958R				
inner primer pair	Parch519 Arch915-GC ^a	25 ^b 95 °C	45 s 52 °C	1 min 72 °C	1 min 30 s Visser et al. (2009)
Fungal 18S rRNA	funSSUF	20 ^b 95 °C	30 s 55 °C	45 s 72 °C	3 min Foster et al. (2013)
outer primer pair	funSSUR				
inner primer pair	FF390 FR1-GC ^a	20 ^b 95 °C	45 s 55 °C	1 min 72 °C	3 min Chu et al. (2011) Brown and Allen-Vercoe (2011)
Archaeal amoA	Arch-amoAF	32 ^b 95 °C	1 min 55 °C	1 min 72 °C	1 min Francis et al. (2005)
	Arch-amoAR				
Bacterial 16S rRNA	28F				
sequencing					
Archaeal 16S rRNA	349F				
sequencing					
Fungal 18S rRNA	funSSUF				
sequencing					
Archaeal amoA	qPCR amoA F	40 95 °C	15 s 55 °C	15 s 72 °C	1 min Bai et al. (2012)
qRT-PCR	qPCR amoA R				

(Dowd et al., 2008) at MR DNA. After removing failed sequence reads, as well as low-quality sequence ends, primers, and chimeras (Gontcharova et al., 2010; Bailey et al., 2010), reads were assembled into clusters using a distributed MegaBLAST.NET algorithm (Dowd et al., 2005), denoised, and compared to the sequences curated by the National Center for Biotechnology Information (NCBI) database library RDP ver 9 (Cole et al., 2009). MegaBLAST outputs were further evaluated using the .NET and C# analysis pipeline (Bailey et al., 2010). Py-rosequence analysis was not normalized for the size of the respective libraries as discussed in McMurdie and Holmes (2014). The identity of each microbial sequence was based on the percentage of the total length of each sequence aligned with the given library database sequence and classified at the appropriate taxonomic levels as previously analyzed (Bailey et al., 2010; Kumar et al., 2012). Sequence data were deposited in the DDBJ Sequence Read Archive (SRA) under study accession number SRP102614. Relative abundance calculations were based on the taxonomic level of order or family.

Amplification of Archaeal *amoA* Gene Sequences

To detect the presence of a putative archaeal *amoA*, genomic DNA samples were amplified by PCR using a primer pair specific for ammonia-oxidizing Archaea (Table 1). The amplification products were visualized after electrophoresis on a 1% agarose gel. After successful detection, semi-quantitative real-time PCR (qRT-PCR) was performed to quantify *amoA* in these samples. First, the PCR products as described above were cloned into pDrive (Qiagen PCR Cloning Kit) and transformed into DH5 α chemically competent *E. coli*. Mini preparations were performed on positive transformants, and isolated plasmids were sequenced (Centre de Recherche du Hospitalier Université Laval [CHUL], St. Foy, Québec, Canada). Standards were prepared by making a dilution series from the original preparation with dilutions ranging from 10⁻¹ to 10⁻⁷. For qRT-PCR, DNA template (5 μ L; control or sample), 10 μ L SYBR Select Master Mix (Life Technologies), 2 μ L sterile water, and 400 nM final concentration of each primer (Table 1) were mixed in an 18 μ L reaction. Thermal cyclers conditions are described in Table 1. Amplifications were analyzed using the Vii a^{TM} 7 Real-Time PCR System (Life Technologies) with a Two-Step, Relative Standard Curve run method and analyzed using the corresponding Vii a^{TM} 7 Software v1.2.4. Each sample was amplified and analyzed in triplicate. The relative abundance of the putative *amoA* gene sequence in each sample was determined by calculating the difference between the C $_t$ value of each unknown and the C $_t$ value of standard controls.

Statistical Analysis

We analyzed overall differences in whole soil core biogeochemistry, microbial biomass, and soluble ions between disturbed and undisturbed cores using non-parametric Mann-Whitney analyses with soil depths assigned as within-core replicates. This approach allowed us to investigate whether within-core variability was less than between-core differences but because of our limited soil core availability, we were not able to test for biogeochemical differences at specific soil depths across sites.

The differences in bacterial, archaeal, and fungal community composition between the disturbed and undisturbed cores were assessed based on relative abundance at the taxonomic level of order, after elimination of all groups with a relative abundance lower than 0.5%. Order (or phylum in certain cases) and family were chosen because each sample was limited to 3000 sequence reads, and we considered that it would be preferable to have greater sequence depth and additional core samples for finer taxonomic resolution. Relative abundance at the level of family is provided for bacterial and fungal sequences (Appendix Figs. A3 and A4). Differences in community composition were examined with non-metric multidimensional scaling (NMS) analyses on a matrix of soil samples by OTUs (level of order) using the Sørensen similarity index in PC-ORD v. 5.0. NMS is a suitable method for assessment because it is applicable to non-linear, non-normally distributed data (McCune et al., 2002), and the data were further evaluated using a non-parametric multi-response permutation procedure (MRPP). In MRPP, the *p*-value represents the likelihood of the observed differences being due to chance. The chance-corrected within-group agreement (“*A*”) represents within-group homogeneity compared to chance alone. “*A*” values range from 0 to 1, where 1 indicates that all samples within a group were identical, and 0 means within-group heterogeneity was equal to expectation by chance (McCune et al., 2002).

The Shannon-Wiener index was used to calculate diversity (“*H*”). “*H*” values were calculated using the raw operational taxonomic unit (OTU) counts for each order. An “*H*” value was calculated for both the disturbed and undisturbed cores and for both the bacterial and fungal communities.

RESULTS

Environmental and Geochemical Characteristics

The environmental and geochemical data for the cores are shown in Table 2. For simplicity and because patterns at the finer depth resolution (every 5 cm) were similar to

TABLE 2

Environmental and geochemical characteristics of core samples taken from an undisturbed (UN) and a disturbed (D) active layer detachment at the Cape Bounty Arctic Watershed Observatory (CBAWO), Melville Island, in the Canadian High Arctic.

Assay ^a	Top ^b		16 cm		26 cm		34 cm	
	UN	D	UN	D	UN	D	UN	D
DOC	23	28	16	18	13	23	13	20
TDN	1.6	2.7	0.9	1.8	0.8	4.7	0.6	4.2
Total C	7	11	8	7	8	8	7	9
Total N	0.7	1.1	0.9	0.7	0.8	0.8	0.7	0.8
C/N	9.8	9.9	8.9	9.7	10.1	10.0	9.7	10.5
MBC	33.6	29.1	13.4	30.8	13.7	22.0	13.6	39.1
MBN	4.4	5.7	2.7	4.1	1.7	3.4	2.2	6.8
MBC/MBN	7.6	5.1	5.0	7.5	8.1	6.6	6.2	5.7
pH	6.1	6.4	6.4	6.4	6.5	6.5	6.3	6.4
Moisture	11.4	25.8	14.0	18.8	10.2	14.8	12.3	12.6
Na ⁺	0.2	5.0	0.2	3.9	0.2	2.9	0.2	3.9
NH ₄ ⁺	neg	neg	neg	neg	neg	0.05	0.01	neg.
K ⁺	0.2	0.3	0.2	0.2	0.3	0.2	0.3	0.1
Mg ²⁺	0.6	0.6	0.3	0.3	0.4	0.2	0.4	0.2
Ca ²⁺	0.8	0.7	0.4	0.5	0.4	0.2	0.5	0.5

^aDissolved organic carbon (DOC), total dissolved nitrogen (TDN), total C (total C), total N (Total N), the carbon:nitrogen ratio (C/N), microbial biomass as assessed by carbon content (MBC), microbial biomass as assessed by nitrogen content (MBN), and the ratio of the latter two measurements (MBC/MBN) are expressed as mg g⁻¹ dry weight of soil. Moisture is gravimetric soil water content expressed as % dryweight. Solute amounts are measured in ppm with neg. indicating that the negligible concentrations were beneath the detection limits of ~0.03 for each solute (with precision corresponding to 1.5%, 27.8%, 6.4%, 1.4%, and 11.1% for Na⁺, NH₄⁺, K⁺, Mg²⁺, and Ca²⁺, respectively).

^bThe top of each core corresponded to 1 cm for the disturbed and 13 cm for the undisturbed core (due to its friable nature, and our consequent inability to recover it from the field).

the patterns shown, only results for the depth for which the DNA was subsequently sequenced are shown.

Within-cores, the “top” soil sample was frequently elevated compared to samples taken at depth in a number of characteristics: for the undisturbed core these included DOC, TDN, MBN, and some ions, and in the disturbed core these included DOC, total C and N, moisture, and some ions. These same characteristics also seemed to vary between the disturbed and undisturbed cores. Overall, across soil depths between cores, a Mann-Whitney U-test indicated that the disturbed core contained significantly greater TDN and Na⁺ pools than the undisturbed core ($W = 26$, $p = 0.03$; and $W = 26$, $p = 0.02$, respectively). DOC and moisture content were relatively more variable across depths within cores thereby only leading to near-tendencies toward overall differences between cores (both: $W = 24$, $p = 0.11$). However, soil moisture, DOC, MBC, and MBN levels all appeared to be higher in the disturbed core relative to the undisturbed core at greater soil depths (26 and 34 cm). In contrast, the other meas-

ured biogeochemical properties varied little, both between depths and between cores, including total C and N, NH₄⁺, K⁺, and pH (Lamhonwah et al., 2016).

DGGE Analysis of Soil Communities

The impact of the active layer detachment on microbial community composition was examined by comparing the DGGE banding patterns of amplified rRNA gene fragments in the disturbed and undisturbed cores. Banding patterns for the bacterial communities revealed some differences, but most bands were seen in all samples (not shown). Upon DGGE analysis following amplification with archaeal 16S rRNA sequence primers many of the bands were similar between the two cores; however, a few differences were noted, including the presence of a band at a depth of 34 cm in the disturbed core (also seen faintly at 26 cm; Appendix Fig. A1). Striking differences were seen after DGGE analysis of the 18S rRNA gene fragments both between the two

cores as well as between depths of the same cores (Fig. 2). For example, different banding patterns were apparent in samples representing the “top” and 5 cm in the disturbed core (Fig. 2), and 4–5 bands are seen in the “top” (1 cm) sample of the disturbed core compared to a single band in the “top” (13 cm) sample of the undisturbed core.

Pyrosequencing Analysis of Soil Communities

Pyrosequencing data indicated similarities in the bacterial community composition between the disturbed and undisturbed cores. For example, the most abundant phylum in every sample in both cores was Actinobacteria, at ~44%, followed by Proteobacteria and Chloroflexi (Fig. 3, part A). Some differences between the disturbed and undisturbed core depths were seen for less abundant orders, which would not have been apparent in the DGGE analysis. For instance, Pseudomonadales and Rhodobacterales were more abundant (~25-fold

and ~26-fold, respectively) in the disturbed core (Fig. 3, part A, boxes), whereas Pseudonocardiales and Rhodocyclales were more plentiful (~48-fold and ~29-fold, respectively) in the undisturbed core (Fig. 3, part A, boxes). The level of diversity, assessed using the Shannon-Wiener index, was similar in the disturbed core and the undisturbed core ($H = 3.01$ and $H = 2.99$, respectively). NMS analysis of the bacterial community composition confirmed a modest shift in the disturbed core compared to the undisturbed core (Fig. 3, part B) with stronger differences in bacterial communities between sites than within sites, even though the latter variation reflects sampling at various soil depths (MRPP, $A = 0.412$, $p = 0.006$). Although there was overall similarity, the changes seen in the bacterial community composition appeared to be driven by increases in soil moisture, DOC, TDN, MBC, and MBN in the disturbed core (Fig. 4, part B). The best fitting NMS solution contained 2-dimensions (final stress = 2.5, final instability = 0.00001, number of iterations = 115). Of note, there was also variability across different depths within the same core, which was most apparent in the disturbed core. For example, there were modest increases in the abundance of Caldilineales and Myxococcales at 26 cm compared to the “top” of the disturbed core (~2-fold for each order). The “top” of the disturbed core also appeared to contain a more even distribution of orders compared to all other depths analyzed.

As anticipated by the few bands seen after DGGE analysis (Appendix Fig. A1), communities amplified using the archaeal primers were not as diverse as bacteria. A single order, Nitrososphaerales, was identified. Of the total reads recovered, there was a greater proportion of Nitrososphaerales in the disturbed core, with a 4-fold greater abundance at 16 cm compared to the undisturbed core (Appendix Fig. A2, box).

The banding differences seen in the fungal DGGE analysis were reflected in the pyrosequencing data displayed to order. The most abundant phylum in both cores was Ascomycota, representing 67% and 83% of all fungal sequences in the disturbed and undisturbed cores, respectively. Chytridiomycota (23%) were more abundant at the “top” of the disturbed core, but not in any of the other samples (Fig. 4, part A, box). A large proportion of sequences from the 34 cm depth sample of the undisturbed core was assigned to an unspecified order (indicating inadequate representation in the database) of the Class Leotiomycetes (Fig. 4, part A, box), and this outlier soil sample had to be removed prior to the NMS analysis (Fig. 4, part B; see text below). Helotiales, which include the ericoid mycorrhizal species in association with some arctic plant species (Walker et al., 2011; Koyama et al., 2014), were present in both cores, but there

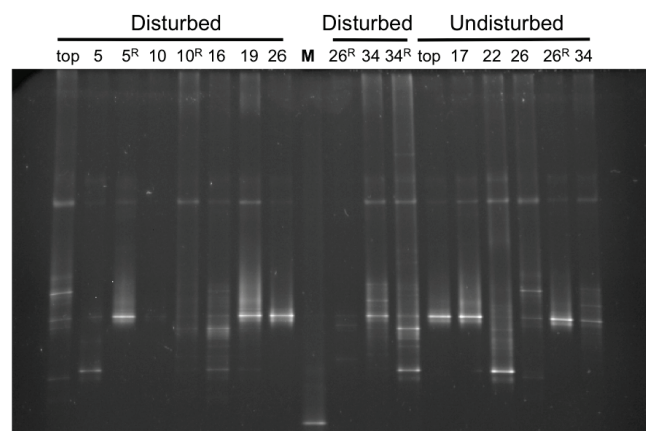


FIGURE 2. Representative gel showing denaturing gradient gel electrophoresis (DGGE) analysis of fungal communities at indicated depths from the disturbed and undisturbed cores. Community composition is based on polymerase chain reaction (PCR) amplification of the 18S rRNA gene fragment. Numbers refer to the core depth of each sample, and were measured from the top of the core. Samples amplified from second, replicate DNA isolations at different depths are indicated by R, which routinely showed identical banding patterns, but with some within-sample heterogeneity. Lane 9 is a DGGE marker (M). DGGE gel was prepared with 8% (w/v) polyacrylamide and a denaturing gradient of 30%–60% denaturing solution. Electrophoresis was performed at 120 V for 5 min, followed by 70 V for 20 h, in 1× Tris-Acetate-EDTA (TAE) buffer at 60 °C. Gels were repeated at least three times; the gel shown is the third gel.

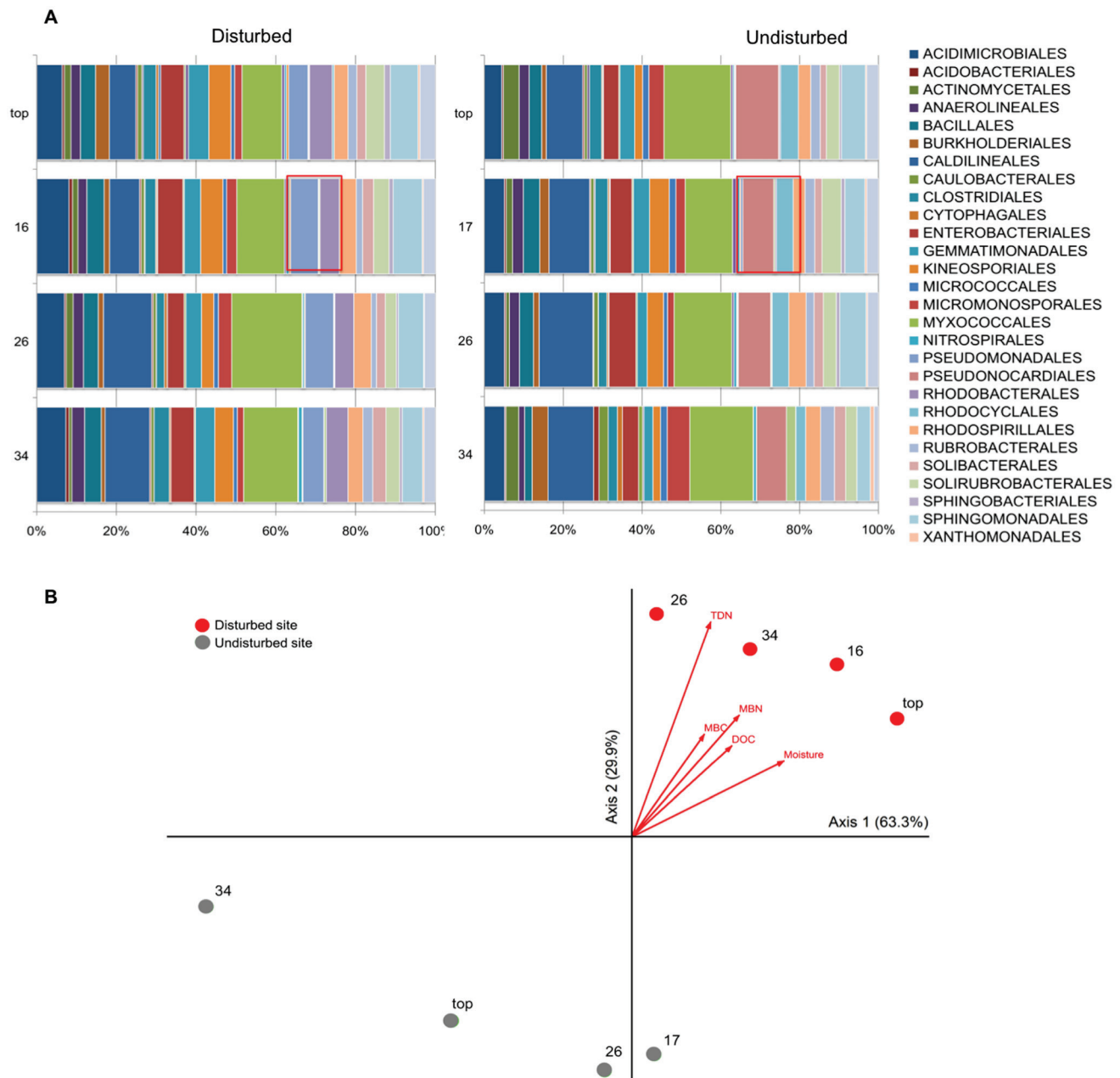


FIGURE 3. Bacterial community composition of the disturbed and undisturbed cores assessed by pyrosequencing. (A) A stacked bar diagram representation of bacterial phylogenetic composition at the taxonomic level of Order for each depth (sample names represent depth in cm) of the disturbed (left) and undisturbed (right) cores. Pyrosequencing was completed in triplicate and thus the stacked bars represent the mean percent abundance. Sequence classification was determined after pyrosequencing of the 16S rRNA gene fragment. The legend shows the 75% most abundant orders, with remaining orders listed from most to least abundant, being Rhizobiales, Acidobacteriales, Xanthomonadales, Nitrosomonadales, Flavobacteriales, Propionibacteriales, Chloroflexales, Desulfobacteriales, and Frankiales. The orders of relative abundance $\leq 0.5\%$ are collectively shown as “Others.” Boxes are referred to in Results. (B) Non-metric multidimensional scaling (NMS) ordination of bacterial communities based on 16S rRNA gene sequences at the taxonomic level of order. Disturbed samples are shown in red and undisturbed samples are shown in gray. Ordination data points represent community profiles from each individual depth sampled (numbers represent depth in cm). The parentheses indicate the variation that can be explained by each ordination axis.

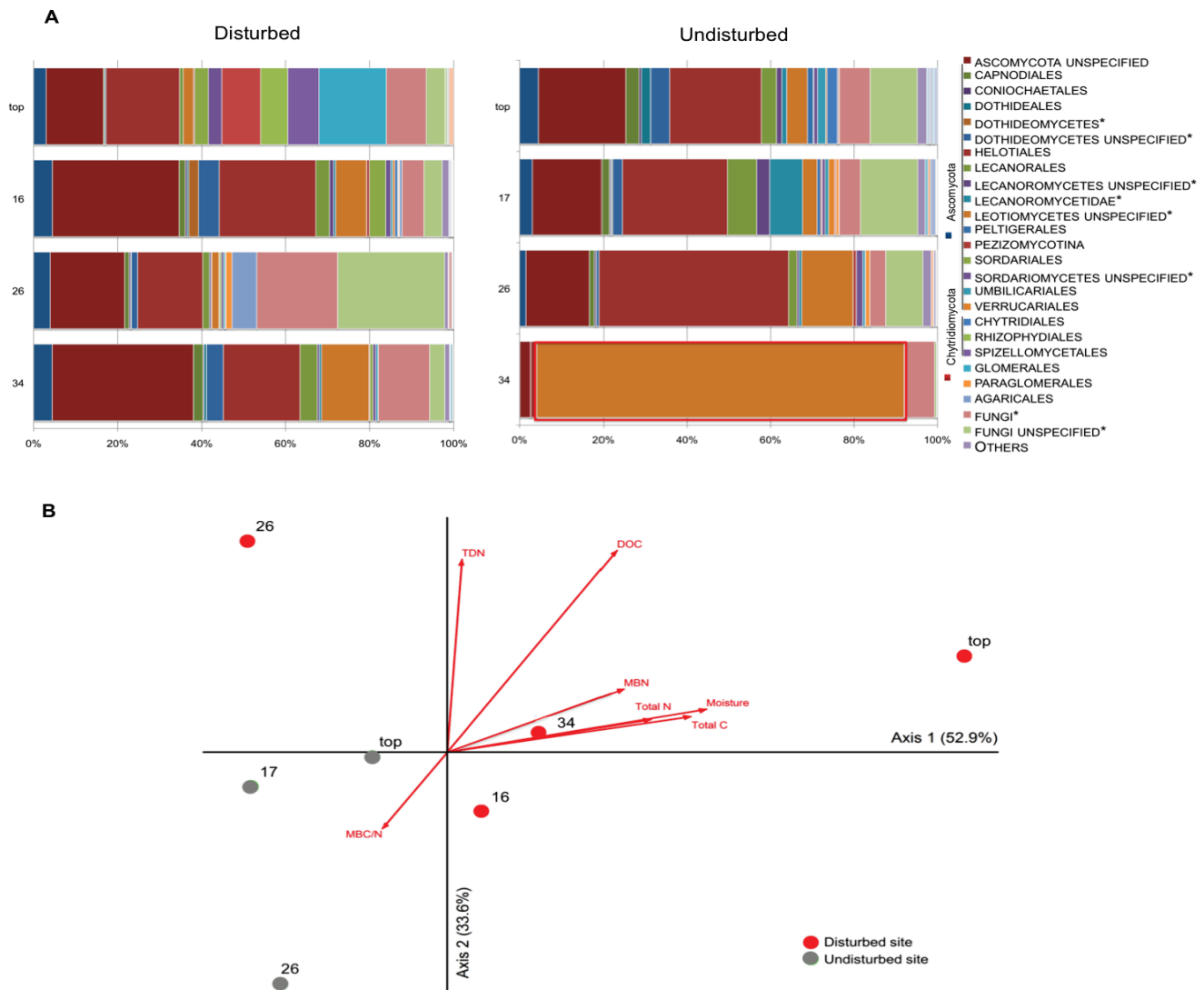


FIGURE 4. Fungal community composition of the disturbed and undisturbed cores assessed by pyrosequencing. (A) Fungal community analysis assessed by pyrosequencing. A stacked bar diagram representation of fungal phylogenetic composition at the taxonomic level of order, if possible, for each depth (sample names represent depth in cm) of the disturbed (left) and undisturbed (right) cores. Sequence classification was determined after pyrosequencing of the 18S rRNA gene fragment. Some fungal sequences shown here could not be classified past the level of phyla (Ascomycota and Chytridiomycota) and class or subclass (asterisks). Pyrosequencing was completed in triplicate and thus the stacked bars represent the mean percent abundance. The legend shows the 75% most abundant orders, with remaining orders listed from most to least abundant being Chaetothyriales, Mycoliciales, Pezizales, Saccharomycetales, Auriculariales, Corticiales, Agyriales, Mucoromycotina, and Microascales. The orders of relative abundance $\leq 0.5\%$ are collectively shown as “Others.” The marked box is referred to in Results. (B) NMS ordination of fungal communities based on 18S rRNA gene sequences at the taxonomic level of order. Samples from the disturbed core are shown in red and from the undisturbed core in gray. Ordination data points represent community profiles from each individual depth sampled (numbers represent depth in cm). The parentheses indicate the variation that can be explained by each ordination axis.

was an overall greater abundance of this order in the undisturbed core, especially in the top three depths. Other orders were more abundant at the “top” of the disturbed core than at any other depth in the disturbed or undisturbed core, including Glomerales (that contain all the

arbuscular mycorrhizal species), Spizellomycetales, and Rhizophydiales. This represents the substantial amount of intra-core variability seen in the fungal communities. It should be noted that because fungi are not extensively documented in this region of the Canadian High Arctic,

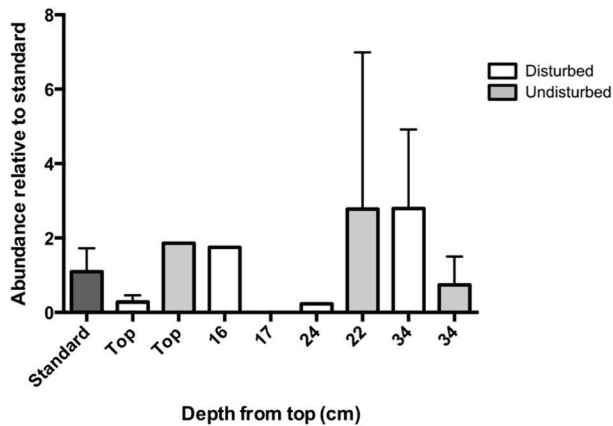


FIGURE 5. Relative abundance of archaeal *amoA* in disturbed and undisturbed samples based on qRT-PCR analysis of *amoA* copy number in samples from indicated depths from the disturbed and undisturbed cores. Abundance in each sample was calculated relative to the standard controls prepared as described in Materials and Methods. Data represent the mean \pm SEM (error bars) of one experiment performed in triplicate.

Figure 4 shows the groupings that best match the literature, which include class, unspecified orders, and phyla. However, only orders were used to calculate the Shannon-Wiener index, to avoid bias. The level of diversity, assessed using the Shannon-Wiener index, showed overall similarity in the disturbed and undisturbed cores ($H = 1.63$ and $H = 1.46$, respectively). NMS indicated a significant shift in community composition between the disturbed and undisturbed soil cores (MRPP, $A = 0.0986$, $p = 0.04$; Fig. 4, part B), and these changes were driven by correlations with TDN, DOC, MBN, moisture, total nitrogen, and total carbon (Fig. 4, part B). The best fitting NMS solution contained 2-dimensions (final stress = 0.1, final instability = 0.05061, number of iterations = 26).

Identification of a Putative Archaeal *amoA* Sequence

PCR amplification using presumptive archaeal *amoA* primers revealed the likely presence of the corresponding gene in both the disturbed and undisturbed cores. An amplified product of 635 bp from both the disturbed and undisturbed cores, showed 91% and 97% identity, respectively, to an *amoA* gene sequence in the database (Accession JQ403672; not shown). Preliminary experiments using PCR amplification followed by assessment of the relative band density following agarose gel analysis suggested that the *amoA* band was more abundant in

the disturbed than undisturbed core (results not shown). When qRT-PCR was employed to confirm these results, there was an apparent increase in the relative abundance of the *amoA* sequence in soil samples from the 16 and 34 cm depth intervals in the disturbed core compared to the corresponding 17 and 34 cm depths in the undisturbed core (Fig. 5).

DISCUSSION

ALDs may be symptomatic of climate change, resulting in altered soil conditions (Lamoureux and Lafrenière, 2009; Pautler et al., 2010). Although the long-term impacts of ALDs are unknown, we postulated that even six years after an ALD event, changes in the composition of the soil microbial communities would reflect this disturbance. Here we show that soluble N pools (TDN) and microbial communities were distinctly different in the two representative cores, supporting the hypothesis, albeit under the limiting sample regime necessitated by severe weather conditions and logistical constraints in the High Arctic.

Generally, High Arctic soil biogeochemical properties (e.g., soluble concentrations and/or pools) decline from the ground surface and down toward the permafrost table at the bottom of the active layer (Christiansen et al., 2012). This pattern was also evident in our undisturbed soil profile where, for example, TDN and DOC were reduced by 63% and 43%, respectively, between the top and bottom samples. By contrast, in the disturbed soil core, several soluble biogeochemical properties either had similar levels throughout the core or decreased more slowly with depth. Surprisingly, not only was overall TDN significantly enhanced in the disturbed soil core relative to the undisturbed core, but TDN also increased by 1.5-fold between the top and bottom soil layer within the disturbed site, suggesting that ALD disturbance events may lead to greater soil N content—not just at the ground surface but also at depth. This change in soil profile soluble N could be because of either physical mixing of soil layers during the permafrost thaw event, downward leaching of solutes, or a combination of the two. TDN comprises both inorganic (ammonium and nitrate) and organic (e.g. amino acids) forms of N. This enhanced nutrient content is likely to affect plant growth and microbial activity as well as potentially reduce soil carbon storage through nutrient priming of organic matter and decomposition thereof (Mack et al., 2004; Nowinski et al., 2008).

Overall, ALD-induced disturbance resulted in no loss of bacterial Shannon-Wiener diversity across depths, but rather a modest change in relative abun-

dance of certain taxonomic orders. These changes in the bacterial community composition in the disturbed core samples correlated with elevated moisture, DOC, and TDN, which are characteristics known to influence microbial activity subsequent to permafrost disturbance (Pautler et al., 2010; Louiseize et al., 2014). Nevertheless, the overall similarity of the bacterial DGGEs and the community structure undoubtedly reflect the same pH and overlying vegetation of the cores (Shi et al., 2015), and additionally provide assurance in the comparison of the paired cores. With respect to intra-core variability, the “top” of the disturbed core appeared to have a more even distribution of bacterial orders than the other depths. The “top” sample contained elevated DOC, TDC, TDN, and moisture and thus may contribute to the observed differences in this sample. Furthermore, DOC and moisture were the most variable; therefore, with respect to biogeochemical factors, these may contribute the most to intra-core variability. The variability of bacterial community composition within the undisturbed core appeared less obvious than the disturbed core, and this may reflect greater stability of the biogeochemical factors, and therefore microbial communities in undisturbed soils.

Archaeal DGGE analysis showed a number of bands, although we did not verify that the amplification products did not include some bacterial sequences. High Arctic archaeal communities are reported to have low diversity (Wilhelm et al., 2011). Notwithstanding this limitation, an obvious difference in archaeal community composition between the two cores was the greater proportion of Nitrososphaerales in all depths of the disturbed core. These are autotrophic ammonia-oxidizing Archaea, the most abundant group of Thaumarcheota in Canadian High Arctic permafrost (Allan et al., 2014). To confirm this observation, we undertook PCR amplification, sequencing, and assessment of *amoA* gene sequence abundance (Fig. 5). Taken together, the sequencing and qRT-PCR results may suggest that ammonia oxidation could increase as a result of ALDs, signaling that additional sites should be examined. If widespread, there would be a potential to alter nitrogen cycling in arctic soils. Ammonium levels were mostly below detection in our soil samples (six out of eight samples across soil cores contained negligible NH_4^+ concentrations), but considering the significant increase in overall soil core TDN at the disturbed site, there might be potential for enhanced ammonia oxidation processes in a continuously changing climate. This is important for our understanding of permafrost disturbances because the oxidation of ammonia decreases nitrogen availability for most plants and soil organisms (Tourna et al., 2008). This in turn results in the release of nitrous oxide to the

atmosphere, which is not only a potent greenhouse gas, but also contributes to ozone depletion (Zhang et al., 2010).

The fungal community appeared more susceptible to disturbance with similar overall diversity but significant changes in some taxa compositions. Although there was considerable variation among depths within each core, statistical analysis revealed even greater variation between the two cores (MRPP, $A = 0.0986$, $p = 0.04$; Fig. 4). Changes to arctic fungal communities have been previously noted in cryoturbated features, including patterned ground, with taxa influenced by soil C, C:N ratio, and soil moisture (Timling et al., 2014). Here, changes in fungal community composition were associated with properties consistent with an ALD including DOC, TDN, MBC, MBN, and enhanced soil moisture, which are factors that have been shown to increase arctic bacterial activity (Pautler et al., 2010), but less is known about eukaryotic consortia including fungi. The relative increase in abundance of Glomerales, Spizellomycetales, and Rhizophydiales in the “top” sample of the disturbed core compared to other depths within the same core may reflect the increase in DOC, TDC, TDN, and moisture at this depth. In addition to changes in the overall fungal assemblage, it was striking that there were almost 20% fewer fungal orders of Ascomycota, an abundant phylum strongly dominated by fungi with filamentous hyphal growth form (Stajich et al., 2009; Koyama et al., 2014) in the disturbed core, compared to the undisturbed core. Furthermore, the Leotiomycetes, an order within the Ascomycota that is completely filamentous in growth form, was particularly abundant in the undisturbed core, especially at 34 cm (Fig. 4, part A). It is known that fungal hyphal networks enhance soil aggregation through physical binding as well as exudations, and contribute to soil stability (Tisdall, 1994; Rillig and Mummey, 2006; Timling et al., 2014). This suggests to us that these networks may help to “hold” active layer soils in a way that fungal species with the unicellular (or yeast-like) growth form cannot. We wonder then if ALDs not only impact microbial communities, but also if fungal communities could influence the likelihood of ALDs?

The answer to this question must await further studies and analyses of other ALDs and their impact on ecosystem properties. It is clear, however, that permafrost disturbance did impact soil communities at this High Arctic site and that the impact was still apparent even after the recovery of the above-ground vegetation. Worryingly, both the relative increased abundance of ammonia-oxidizing Archaea, and the reduction of hyphal

fungi that may stabilize soils, could exacerbate high-latitude landscape changes associated with climate change and increased seasonal warming.

ACKNOWLEDGMENTS

This work was supported by funding from the Natural Sciences and Engineering Research Council (NSERC) of Canada and Arctic Development and Adaptation to Permafrost in Transition (ADAPT) program, ArcticNet Network Centres of Excellence, and NSERC Discovery grants to P. Grogan, S. F. Lamoureux, M. J. Lafrenière, and V. K. Walker. Polar Continental Shelf Programme provided logistics for field sampling.

REFERENCES CITED

- Abrams, E. S., and Stanton, V. P., Jr., 1992: Use of denaturing gradient gel electrophoresis to study conformational transitions in nucleic acids. *Methods in Enzymology*, 212: 71–104, doi: [http://dx.doi.org/10.1016/0076-6879\(92\)12006-c](http://dx.doi.org/10.1016/0076-6879(92)12006-c).
- Allan, J., Ronholm, J., Mykytczuk, N., Greer, C., Onstott, T., and Whyte, L., 2014: Methanogen community composition and rates of methane consumption in Canadian High Arctic permafrost soils. *Environmental Microbiology Reports*, 6: 136–144, doi: <http://dx.doi.org/10.1111/1758-2229.12139>.
- Bai, Y., Sun, Q., Wen, D., and Tang, X., 2012: Abundance of ammonia-oxidizing bacteria and archaea in industrial and domestic wastewater treatment systems. *FEMS Microbiology Ecology*, 80: 323–330, doi: <http://dx.doi.org/10.1111/j.1574-6941.2012.01296.x>.
- Bailey, M. T., Dowd, S. E., Parry, N. M., Galley, J. D., Schauer, D. B., and Lyte, M., 2010: Stressor exposure disrupts commensal microbial populations in the intestines and leads to increased colonization by *Citrobacter rodentium*. *Infection and Immunity*, 78: 1509–1519, doi: <http://dx.doi.org/10.1128/iai.00862-09>.
- Boon, N., Windt, W., Verstraete, W., and Top, E. M., 2002: Evaluation of nested PCR-DGGE (denaturing gradient gel electrophoresis) with group-specific 16S rRNA primers for the analysis of bacterial communities from different wastewater treatment plants. *FEMS Microbiology Ecology*, 39: 101–112, doi: <http://dx.doi.org/10.1111/j.1574-6941.2002.tb00911.x>.
- Bosquet, L. M., 2011: *The Effects of Observed and Experimental Climate Change and Permafrost Disturbance on Tundra Vegetation in the Western Canadian High Arctic*. Master's thesis, Queen's University, Kingston, Ontario, 114 pp.
- Brookes, P., Kragt, J. F., Powlson, D. S., and Jenkinson, D. S., 1985: Chloroform fumigation and the release of soil nitrogen: the effects of fumigation time and temperature. *Soil Biology and Biochemistry*, 17: 831–835, doi: [http://dx.doi.org/10.1016/0038-0717\(85\)90143-9](http://dx.doi.org/10.1016/0038-0717(85)90143-9).
- Brown, E., and Allen-Vercoe, E., 2011: Analysis of the fungal, archaeal and bacteriophage diversity in the human distal gut. *Studies by Undergraduate Researchers at Guelph*, 4: 75–82.
- Buckeridge, K. M., and Grogan, P., 2010: Deepened snow increases late thaw biogeochemical pulses in mesic low arctic tundra. *Biogeochemistry*, 101: 105–121, doi: <http://dx.doi.org/10.1007/s10533-010-9426-5>.
- Buckeridge, K. M., Banerjee, S., Siciliano, S. D., and Grogan, P., 2013: The seasonal pattern of soil microbial community structure in mesic Low Arctic tundra. *Soil Biology & Biochemistry*, 65: 338–347, doi: <http://dx.doi.org/10.1016/j.soilbio.2013.06.012>.
- Christiansen, C. T., Svendsen, S. H., Schmidt, N. M., and Michelsen, A., 2012: High arctic heath soil respiration and biogeochemical dynamics during summer and autumn freeze-in—Effects of long-term enhanced water and nutrient supply. *Global Change Biology*, 18(10): 3224–3236, doi: <http://dx.doi.org/10.1111/j.1365-2486.2012.02770.x>.
- Chu, H., Neufeld, J. D., Walker, V. K., and Grogan, P., 2011: The influence of vegetation type on the dominant soil bacteria, archaea, and fungi in a low arctic tundra landscape. *Soil Science Society of America Journal*, 75: 1756–1765, doi: <http://dx.doi.org/10.2136/sssaj2011.0057>.
- Cole, J. R., Wang, Q., Cardenas, E., Fish, J., Chai, B., Farris, R. J., Kulam-Syed-Mohideen, A. S., McGarrell, D. M., Marsh, T., Garrity, G. M., and Tiedje, J. M., 2009: The ribosomal database project: improved alignments and new tools for rRNA analysis. *Nucleic Acids Research*, 37: D141–D145, doi: <http://dx.doi.org/10.1093/nar/gkn879>.
- Delidow, B. C., Lynch, J. P., Peluso, J. J., and White, B. A., 1993: Polymerase chain reaction: basic protocols. In White, B. A. (ed.), *PCR Protocols: Current Methods and Applications*. New York: Humana Press.
- Dowd, S. E., Zaragoza, J., Rodriguez, J. R., Oliver, M. J., and Payton, P. R., 2005: Windows .NET network distributed basic local alignment search toolkit (W.ND-BLAST). *BMC Bioinformatics*, 6: 93, doi: <http://dx.doi.org/10.1186/1471-2105-6-93>.
- Dowd, S. E., Callaway, T. R., Wolcott, R. D., Sun, Y., McKeenan, T., Hagevoort, R. G., and Edrington, T. S., 2008: Evaluation of the bacterial diversity in the feces of cattle using 16S rDNA bacterial tag-encoded FLX amplicon pyrosequencing (bTEFAP). *BMC Microbiology*, 8: 125, doi: <http://dx.doi.org/10.1186/1471-2180-8-125>.
- Foster, M. L., Dowd, S. E., Stephenson, C., Steiner, J. M., and Suchodolski, J. S., 2013: Characterization of the fungal microbiome (mycobiome) in fecal samples from dogs. *Veterinary Medicine International*, 2013: 658373, doi: <http://dx.doi.org/10.1155/2013/658373>.
- Francis, C. A., Roberts, K. J., Beman, J. M., Santoro, A. E., and Oakley, B. B., 2005: Ubiquity and diversity of ammonia-oxidizing archaea in water columns and sediments of the ocean. *Proceedings of the National Academy of Sciences of the United States of America*, 102: 14683–14688, doi: <http://dx.doi.org/10.1073/pnas.0506625102>.
- Fujimura, K. E., and Egger, K. N., 2012: Host plant and environment influence community assembly of High

- Arctic root-associated fungal communities. *Fungal Ecology*, 5: 409–418.
- Geml, J., Morgado, L. N., Semenova, T. A., Welker, J. M., Walker, M. D., and Smets, E., 2015: Long-term warming alters richness and composition of taxonomic and functional groups of arctic fungi. *FEMS Microbiology Ecology*, 91(8): fiv095, doi: <http://dx.doi.org/10.1093/femsec/fiv095>.
- Gontcharova, V., Youn, E., Wolcott, R. D., Hollister, E. B., Gentry, T. J., and Dowd, S. E., 2010: Black Box Chimera Check (B2C2): a Windows-based software for batch depletion of chimeras from bacterial 16S rRNA gene datasets. *The Open Microbiology Journal*, 4: 47–52, doi: <http://dx.doi.org/10.2174/1874285801004010047>.
- IPCC, 2007: Climate change 2007: the physical science basis. In Solomon, S., Qin, D., Manning, M., Chen, Z., Marquis, M., Averyt, K. B., Tignor, M., and Miller, H. L. (eds.), *Contribution of Working Group I to the Fourth Assessment Report of the Intergovernmental Panel on Climate Change*. Cambridge and New York: Cambridge University Press, 1–383.
- Jones, B. M., Amundson, C. L., and Koch, J. C., 2013: Thermokarst and thaw-related landscape dynamics: an annotated bibliography with an emphasis on potential effects on habitat and wildlife. *U.S. Geological Survey Open-File Report 2013-1161*.
- Kokelj, S. V., and Burn, C. R., 2005: Geochemistry of the active layer and near-surface permafrost, Mackenzie delta region, Northwest Territories, Canada. *Canadian Journal of Earth Sciences*, 42: 37–48, doi: <http://dx.doi.org/10.1139/e04-089>.
- Koyama, A., Wallenstein, M. D., Simpson, R. T., and Moore, J. C., 2014: Soil bacterial community composition altered by increased nutrient availability in arctic tundra soils. *Frontiers in Microbiology*, 5: 516, doi: <http://dx.doi.org/10.3389/fmicb.2014.00516>.
- Kumar, N., Grogan, P., Chu, H., Christiansen, C. T., and Walker, V. K., 2012: The effect of freeze-thaw conditions on arctic soil bacterial communities. *Biology*, 2: 356–377, doi: <http://dx.doi.org/10.3390/biology2010356>.
- Kuo, S., 1996: Phosphorus. In *Methods of Soil Analysis. Part 3: Chemical Methods*. Madison, Wisconsin: Soil Science Society of America and American Society of Agronomy, 869–919.
- Lamhonwah, D., Lafrenière, M. J., Lamoureux, S. F., and Wolfe, B. B., 2016: Multi-year impacts of permafrost disturbance and thermal perturbation on High Arctic stream chemistry. *Arctic Science*, 3(2): 1–23, doi: <https://dx.doi.org/10.1139/as-2016-0024>.
- Lamoureux, S. F., and Lafrenière, M. J., 2009: Fluvial impact of extensive active layer detachments, Cape Bounty, Melville Island, Canada. *Arctic, Antarctic, and Alpine Research*, 41: 59–68, doi: [http://dx.doi.org/10.1657/1938-4246\(08-030\)](http://dx.doi.org/10.1657/1938-4246(08-030)).
- Lewis, T., and Lamoureux, S. F., 2010: Twenty-first century discharge and sediment yield predictions in a small High Arctic watershed. *Global Planet Change*, 71: 27–41, doi: <http://dx.doi.org/10.1016/j.gloplacha.2009.12.006>.
- Lewis, T., Lafrenière, M. J., and Lamoureux, S. F., 2012: Hydrochemical and sedimentary responses of paired High Arctic watersheds to unusual climate and permafrost disturbance, Cape Bounty, Melville Island, Canada. *Hydrological Processes*, 26: 2003–2018, doi: <http://dx.doi.org/10.1002/hyp.8335>.
- Louiseize, N. L., Lafrenière, M. J., and Hastings, M. G., 2014: Stable isotopic evidence of enhanced export of microbially derived nitrate following active layer slope disturbance in the Canadian High Arctic. *Biogeochemistry*, 121: 565–580, doi: <http://dx.doi.org/10.1007/s10533-014-0023>.
- Mack, M. C., Schuur, E. G., Bret-Harte, M. S., Shaver, G. R., and Chapin, F. S., 2004: Ecosystem carbon storage in arctic tundra reduced by long-term nutrient fertilization. *Nature*, 431: 440–443, doi: <http://dx.doi.org/10.1038/nature02887>.
- McCune, B., Grace, J. B., and Urban, D. L., 2002: *In Analysis of Ecological Communities*. Glenden Beach, Oregon: MjM Software.
- McMurdie, P. J., and Holmes, S., 2014: Waste not, want not: why rarefying microbiome data is inadmissible. *PLoS Computational Biology*, 10(4): e1003531, doi: <https://dx.doi.org/10.1371/journal.pcbi.1003531>.
- Mulvaney, R., 1996: Nitrogen-inorganic forms. In *Methods of Soil Analysis. Part 3: Chemical Methods*. Madison, Wisconsin: Soil Science Society of America and American Society of Agronomy, 1123–1184.
- Muyzer, G., de Waal, E. C., and Uitterlinden, A. G., 1993: Profiling of complex microbial populations by denaturing gradient gel electrophoresis analysis of polymerase chain reaction-amplified genes coding for 16S rRNA. *Applied and Environmental Microbiology*, 59: 695–700.
- Myers, R. M., Sheffield, V., and Cox, D. R., 1988: Detection of single base changes in DNA: ribonuclease cleavage and denaturing gradient gel electrophoresis. In Davies, K. E. (ed.), *Genome Analysis: a Practical Approach*. Oxford, England: IRL Press Limited, 95–139.
- Nelson, D. W., and Sommers, L. E., 1996: Total carbon, organic carbon and organic matter. In *Methods of Soil Analysis. Part 3: Chemical Methods*. Madison, Wisconsin: Soil Science Society of America and American Society of Agronomy, 961–1010.
- Nowinski, N., Trumbore, S., Schuur, E. G., Mack, M., and Shaver, G., 2008: Nutrient addition prompts rapid destabilization of organic matter in an arctic tundra ecosystem. *Ecosystems*, 11: 16–25, doi: <http://dx.doi.org/10.1007/s10021-007-9104-1>.
- Øvreås, L., Forney, L., Daae, F. L., and Torsvik, V., 1997: Distribution of bacterioplankton in meromictic Lake Saelenvannet, as determined by denaturing gradient gel electrophoresis of PCR-amplified gene fragments coding for 16S rRNA. *Applied and Environmental Microbiology*, 63: 3367–3373.
- Pautler, B. G., Simpson, A. J., McNally, D. J., Lamoureux, S. F., and Simpson, M. J., 2010: Arctic permafrost active layer detachments stimulate microbial activity and degradation of soil organic matter. *Environmental Science and Technology*, 44: 4076–4082, doi: <http://dx.doi.org/10.1021/es903685j>.

- Rillig, M. C., and Mummey, D. L., 2006: Mycorrhizas and soil structure. *New Phytologist*, 171: 41–53, doi: <http://dx.doi.org/10.1111/j.1469-8137.2006.01750.x>.
- Schadt, C. W., Martin, A. P., Lipson, D. A., and Schmidt, S. K., 2003: Seasonal dynamics of previously unknown fungal lineages in tundra soils. *Science*, 301: 1359–1361, doi: <http://dx.doi.org/10.1126/science.1086940>.
- Shi, Y., Xiang, X., Shen, C., Chu, H., Neufeld, J. D., Walker, V. K., and Grogan, P., 2015: Vegetation-associated impacts on arctic tundra bacterial and microeukaryotic communities. *Applied and Environmental Microbiology*, 81: 492–501.
- Stajich, J. E., Berbee, M. L., Blackwell, M., Hibbett, D. S., James, T. Y., Spatafora, J. W., and Taylor, J. W., 2009: The fungi. *Current Biology*, 19: R840–5, doi: <http://dx.doi.org/10.1016/j.cub.2009.07.004>.
- Steven, B., Briggs, G., McKay, C. P., Pollard, W. H., Greer, C. W., and Whyte, L. G., 2007: Characterization of the microbial diversity in a permafrost sample from the Canadian High Arctic using culture-dependent and culture-independent methods. *FEMS Microbiology Ecology*, 59: 513–523, doi: <http://dx.doi.org/10.1111/j.1574-6941.2006.00247.x>.
- Timling, I., and Taylor, D. L., 2012: Peeking through a frosty window: molecular insights into the ecology of arctic soil fungi. *Fungal Ecology*, 5: 419–429, doi: <http://dx.doi.org/10.1016/j.funeco.2012.01.009>.
- Timling, I., Walker, D. A., Nusbaum, C., Lennon, N. J., and Taylor, D. L., 2014: Rich and cold: diversity, distribution and drivers of fungal communities in patterned-ground ecosystems of the North American Arctic. *Molecular Ecology*, 23: 3258–3272, doi: <http://dx.doi.org/10.1111/mec.12743>.
- Tisdall, J. M., 1994: Possible role of soil microorganisms in aggregation in soils. *Plant and Soil*, 159: 115–121.
- Tourna, M., Freitag, T. E., Nicol, G. W., and Prosser, J. I., 2008: Growth, activity and temperature responses of ammonia-oxidizing archaea and bacteria in soil microcosms. *Environmental Microbiology*, 10: 1357–1364, doi: <http://dx.doi.org/10.1111/j.1462-2920.2007.01563.x>.
- Vissers, E. W., Bodelier, P. L., Muyzer, G., and Laanbroek, H. J., 2009: A nested PCR approach for improved recovery of archaeal 16S rRNA gene fragments from freshwater samples. *FEMS Microbiology Letters*, 298: 193–198, doi: <http://dx.doi.org/10.1111/j.1574-6968.2009.01718.x>.
- Wagner, D., 2008: Microbial communities and processes in arctic permafrost environments. *Soil Biology*, 13: 133–154.
- Walker, J. F., Aldrich-Wolfe, L., Riffel, A., Barbare, H., Simpson, N. B., Trowbridge, J., and Jumpponen, A., 2011: Diverse Helotiales associated with the roots of three species of arctic Ericaceae provide no evidence for host specificity. *New Phytologist*, 191: 515–527, doi: <http://dx.doi.org/10.1111/j.1469-8137.2011.03703.x>.
- Wilhelm, R. C., Niederberger, T. D., Greer, C., and Whyte, L. G., 2011: Microbial diversity of active layer and permafrost in an acidic wetland from the Canadian High Arctic. *Canadian Journal of Microbiology*, 57: 303–315, doi: <http://dx.doi.org/10.1139/W11-004>.
- Yergeau, E., Hogues, H., Whyte, L. G., and Greer, C. W., 2010: The functional potential of High Arctic permafrost revealed by metagenomic sequencing, qPCR and microarray analyses. *International Society for Microbial Ecology Journal*, 4: 1206–1214, doi: <http://dx.doi.org/10.1038/ismej.2010.41>.
- Zhang, L., Offre, P. R., He, J., Verhamme, D. T., Nicol, G. W., and Prosser, J. I., 2010: Autotrophic ammonia oxidation by soil thaumarchaea. *Proceedings of the National Academy of Sciences of the United States of America*, 107: 17240–17245, doi: <http://dx.doi.org/10.1073/pnas.1004947107>.

MS submitted 13 October 2016

MS accepted 30 May 2017

APPENDIX

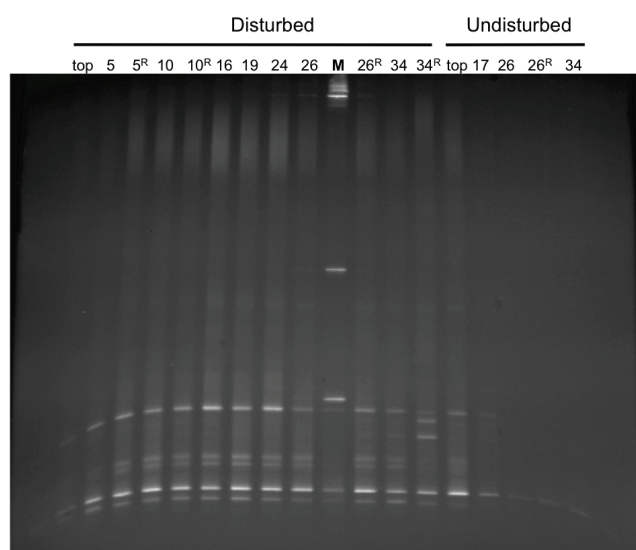


FIGURE A1. Representative gel showing DGGE analysis of communities amplified by archaeal primers at indicated depths from the disturbed and undisturbed cores. Community composition is based on PCR amplification of the 16S rRNA gene fragment. Numbers refer to the core depth of each sample, and were measured from the top of the core. Samples amplified from second, replicate DNA isolations at different depths are indicated by R, which frequently showed identical banding patterns but not always and thus reflect some within-sample heterogeneity. Lane 10 is a 1 kb ladder used as a marker (M). DGGE gels were prepared with 8% (w/v) polyacrylamide and a denaturing gradient of 40%–70% denaturing solution. Electrophoresis was performed at 120 V for 5 min, followed by 70 V for 20 h, in 1× TAE buffer at 60 °C. Gels were repeated at least three times; the gel shown is the fifth gel.

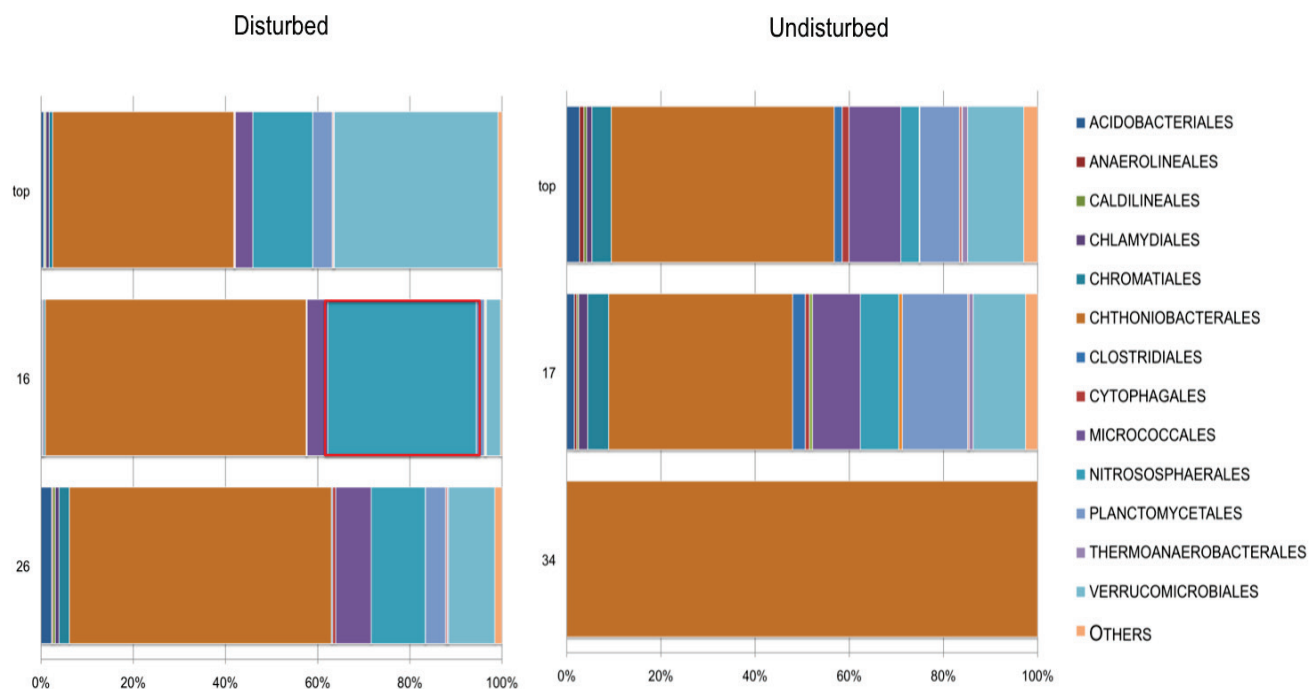


FIGURE A2. Community composition of the disturbed and undisturbed cores assessed by pyrosequencing using recommended archaeal primers (see Table 1). A stacked bar diagram representation of the phylogenetic composition at the taxonomic level of order for each depth (sample names represent depth in cm) of the disturbed (left) and undisturbed (right) cores using primers thought to be relatively specific for archaeal sequences. Pyrosequencing was completed in triplicate and thus the stacked bars represent the mean percent abundance. Sequence classification was determined after pyrosequencing of the 16S rRNA gene fragment. The legend shows the 75% most abundant orders including bacteria, which were sequenced with the primers, with remaining orders listed from most to least abundant, being Rhodocyclales, Oceanospirillales, Desulfuromonadales, and Spartobacteriales. The orders of relative abundance $\leq 0.5\%$ are collectively shown as “Others.” The box is referred to in Results.

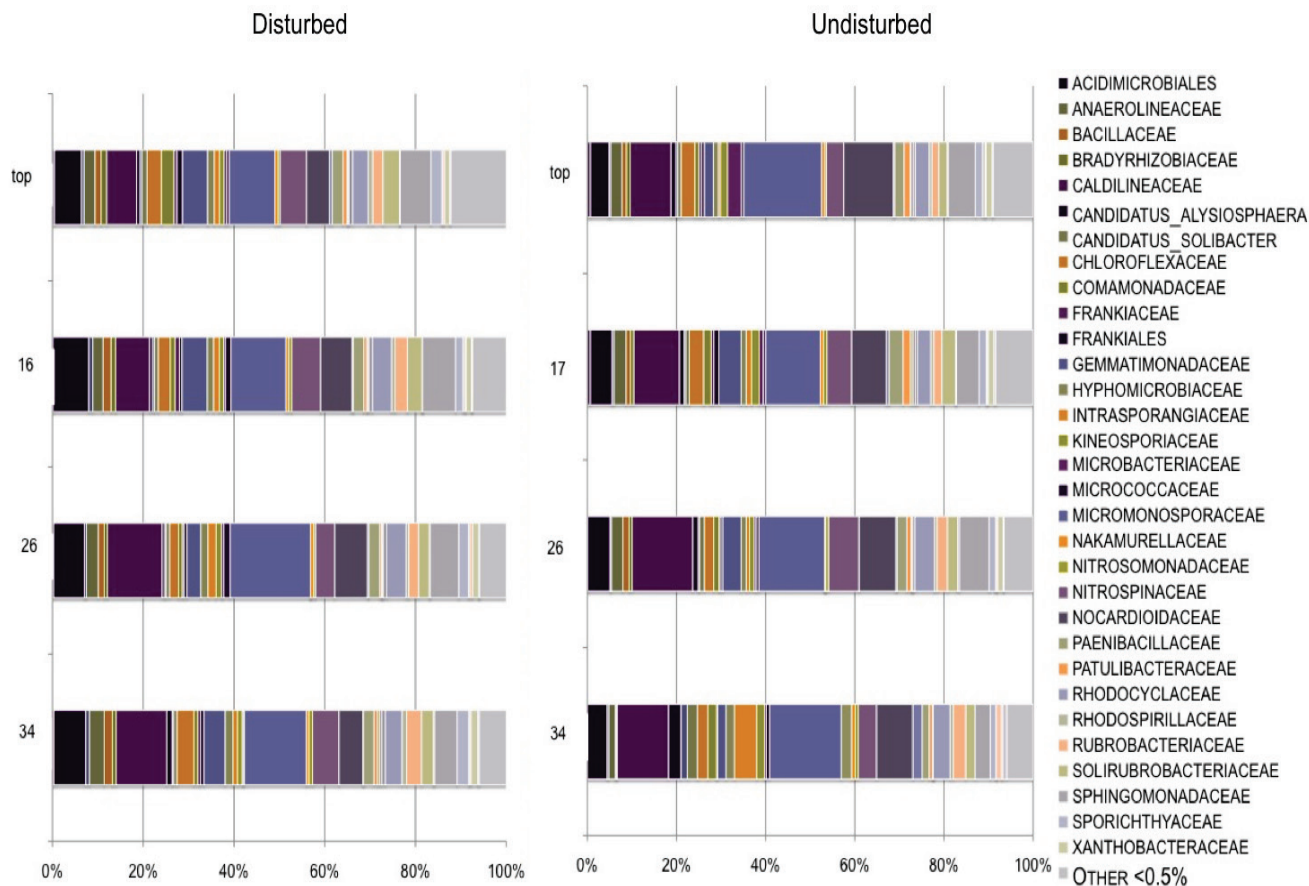


FIGURE A3. Bacterial community composition of the disturbed and undisturbed cores assessed by pyrosequencing and displayed at the taxonomic level of family. A stacked bar diagram representation of bacterial phylogenetic composition at the taxonomic level of family for each depth (sample names represent depth in cm) of the disturbed (left) and undisturbed (right) cores. Pyrosequencing was completed in triplicate and thus the stacked bars represent the mean percent abundance. Sequence classification was determined after pyrosequencing of the 16S rRNA gene fragment. The legend shows the 50% most abundant families. The families of relative abundance $\leq 0.5\%$ are collectively shown as “Others.”

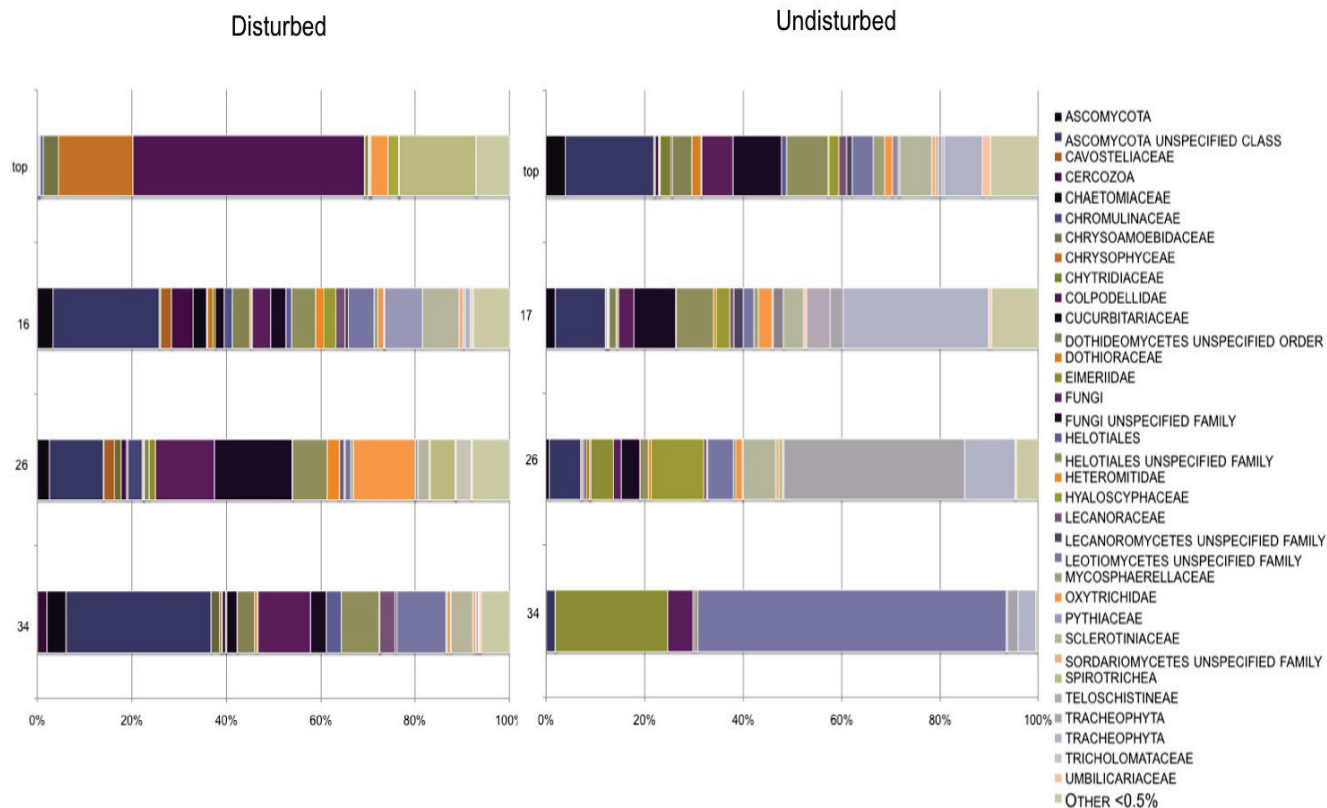


FIGURE A4. Fungal community composition of the disturbed and undisturbed cores assessed by pyrosequencing and displayed at the taxonomic level of family. A stacked bar diagram representation of fungal phylogenetic composition at the taxonomic level of family for each depth (sample names represent depth in cm) of the disturbed (left) and undisturbed (right) cores. Pyrosequencing was completed in triplicate and thus the stacked bars represent the mean percent abundance. Sequence classification was determined after pyrosequencing of the 18S rRNA gene fragment. The legend shows the 50% most abundant families. The families of relative abundance $\leq 0.5\%$ are collectively shown as “Others.”